Elastocaloric effect in Cu-Zn-Al

Author: Daniel Vega Vega
Advisor: Lluís Mañosa Carrera
Facultat de Física, Universitat de Barcelona, Diagonal 645, 08028 Barcelona, Spain.*

Abstract: This work aims to study the elastocaloric effect in a Cu-Al-Zn shape memory alloy sample. The elastocaloric effect refers to the reversible thermal response (isothermal entropy change, or adiabatic temperature change) of a body when subjected to a uniaxial stress. To measure the entropy change of the martensitic transformation, differential scanning calorimetry technique has been used. The calorimeter is capable to work under magnetic fields and the calibration of the calorimetric system is also presented. We obtain a maximum value for the stress-induced entropy change of 22,35 J/kg·K^{-1} within the temperature range between 32ºC and 41ºC and an applied stress of 32,17 MPa.

I. INTRODUCTION

Cu-Zn-Al alloys belong to the family of shape memory alloys which undergo a structural (martensitic transition) from a high temperature ordered cubic phase towards a monoclinic low temperature phase. They can recover from very large deformations (10%) by simply changing its temperature (shape memory effect). While the volume change of the transformation is negligibly small, the transition involves a large shear strain (along the <110> directions), and therefore application of uniaxial stress drives the material from the cubic to the monoclinic phase. The transition encompasses a large entropy change which is the responsible of the large elastocaloric effect in these materials.

A caloric effect associated with a change of a field **Y** is quantified by

$$\Delta S(0 \to \boldsymbol{Y}) = \int_0^Y \left(\frac{\partial x}{\partial T}\right)_Y dY \tag{1}$$

when the field is applied isothermally, and

$$\Delta T(0 \to \boldsymbol{Y}) = -\int_0^Y \frac{T}{C}\left(\frac{\partial x}{\partial T}\right)_Y dY \tag{2}$$

when the field is applied adfiabatically.

In the particular case of the elastocaloric effect, the field is a uniaxial tensile stress σ for which the corresponding displacement is the strain ε (relative elongation along the direction of the applied force). The above expressions also quantify the magnetocaloric (Y=H and x=M), barocaloric (Y=-p and x=V) and electrocaloric (Y=E and x=P) effects, where H is the magnetic field, M, magnetization, p hydrostatic pressure, V, volume, E, electric field and P, polarization.

First-order phase transitions are defined to be those that, in the vicinity of the transition temperature T_c, involve a non-zero latent heat and have associated sudden jump in the entropy of the system. Clausius-Clapeyron equation define the coexistence curve of an ideal first-order phase transition. The pair of conjugate variables that involve our study leads to the followingt expression for the C-C equation

$$\frac{dT}{d\sigma} = \frac{1}{\rho}\frac{\Delta\varepsilon}{\Delta S} \tag{3}$$

which shows the shift of the transition temperature T_c as a function of the stress σ, where ρ is the density of the material.

Differential scanning calorimetry (DSC) is the best suited calorimetric technique to determine entropy change for first-order phase transitions. In a DSC, the heat released by the sample is recorded as a function of temperature, from which the entropy is obtained as:

$$S(T,\sigma) - S(T_0,\sigma) = \int_{T_0}^{T} \frac{1}{T}\frac{dQ/dt}{dT/dt}dT \tag{4}$$

where dQ/dT is the heat flux and dT/dt is the heating (or cooling) rate. The field-induced entropy-change, $\Delta S(T,\sigma)$, is obtained by subtracting the integrated curves.
The elastocaloric effect is then calculated as:

$$\Delta S(T,\sigma) = S(T,\sigma) - S(T,0) \tag{5}$$

II. EXPERIMENTAL DETAILS

A. Calorimeter

A differential calorimeter basically operates measuring the temperature difference between the sample under study (S) and an inert reference (R). Sample and reference need to be in the same conditions for a proper measurement of the heat flux, this involves special symmetry conditions for the design of a calorimeter in order to ensure similar heat transfer conditions and that external perturbations affect similarly both sample and reference. One of the specific features of our calorimeter is that is designed to support magnetic fields and uniaxial stress over the sample. When the temperature of the calorimetric block is continuously changed, the calorimeter is called differential scanning calorimeter (DSC). Our analysis will be restricted to the quasi-static approximation so that the sample has to be able to follow the temperature profile of the calorimetric block minimizing temperature gradients.

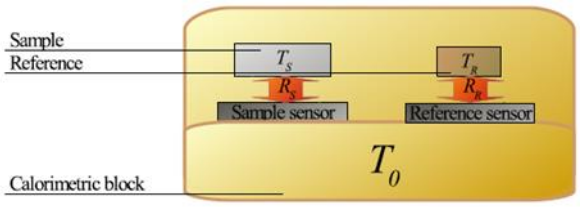

Fig. 1 Sketch of a DSC setup extracted from [3] where R represents the thermal resistance of the medium and $T_S, T_{R,} T_0$, the temperatures of the sample, reference and calorimetric block respectively.

The structure of the calorimeter is built from copper block which ensures a proper thermal inertia of the system. The reference is also made of copper with a mass similar to that of the sample. Both sample and reference are placed on a pair of differentially connected thermobatteries which act as temperature sensors. One face of each thermobattery is in contact with the calorimetric block and the other face holds either the copper reference or the sample. There is an aluminium disc between the sample and the thermobattery supported by a plastic structure to prevent the thermobattery broke when stress is applied to the sample. The thermal contact conditions are improved with silicone heat conductive paste. Due to thermoelectric effect, each thermobattery provides a voltage output. The electric output of the calorimeter, Y, is proportional to the temperature difference between sample and reference and the thermobatteries are connected differentially so that the final voltage output is $Y = V_S - V_R = B(T_S - T_R)$. The sensitivity $S = BR = \Delta Y/P$, where P is the dissipated power, is a characteristic feature of the calorimeter and is obtained by calibration procedures. The calorimeter temperature T_0 is read with a Pt-100 platinum resistance embedded in the middle of the calorimetric block.

B. Calibration

The sensitivity is the ratio between the calorimetric signal and the heat flux. Due to the semiconducting nature of the sensors, the sensitivity of the calorimeter changes with temperature. To measure the sensitivity, the circuit shown in Fig 2. is mounted.

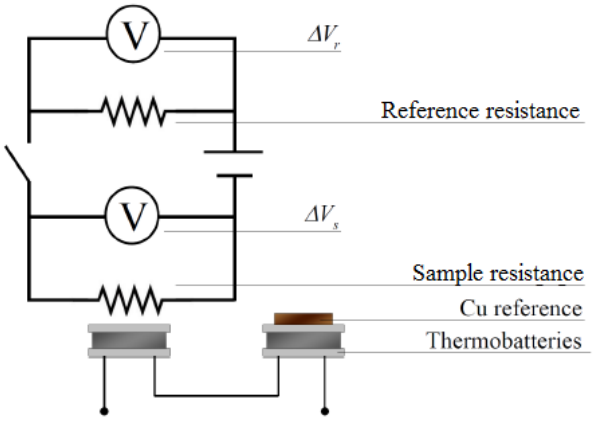

Fig. 2 Sketch of the electrical circuit for the calibration of the calorimeter extracted from [3]

The sample has been replaced by a 120 Ω resistance inside a small copper block and it is connected in series with another resistance of 100 Ω (reference resistance) and a power supply. The reason of the reference resistance is to determine the exact intensity, otherwise, only with the internal one, intensity will change for different temperatures. Two different voltmeters give us the reading of the voltages for the sample resistance, V_s, and the reference resistance, V_r. Reference resistance ($R_{r)}$ is limited to a 100mA intensity and the sample resistance (R_s) has a released power limit of 0,25W. Through Ohm's law $V = I(R_s + R_r)$ and Joule's effect $P = V_r I$ an electric voltage of 9V is deduced to keep our components safe, where $V = V_s + V_r$. When the system is at a stable T, provided by *Lauda Proline* thermal bath, the 9V electric voltage is applied by the power supply closing the circuit, and when the electric signal is stable, the voltage is removed opening the circuit.

The calorimetric signal is recorded as a function of time for different temperatures in the operational range. Then the sensitivity can be calculated as

$$S = \frac{\Delta Y \cdot R_r}{V_s V_r}$$

where ΔY is the height difference of the calorimeter signal when voltage is applied and a baseline extrapolated from the region without voltage.

C. Experimental setup & procedure

The experimental setup, represented in Fig. 3, can simultaneously perform both calorimetry and dilatometry measurements under applied magnetic fields and uniaxial compressive stresses.

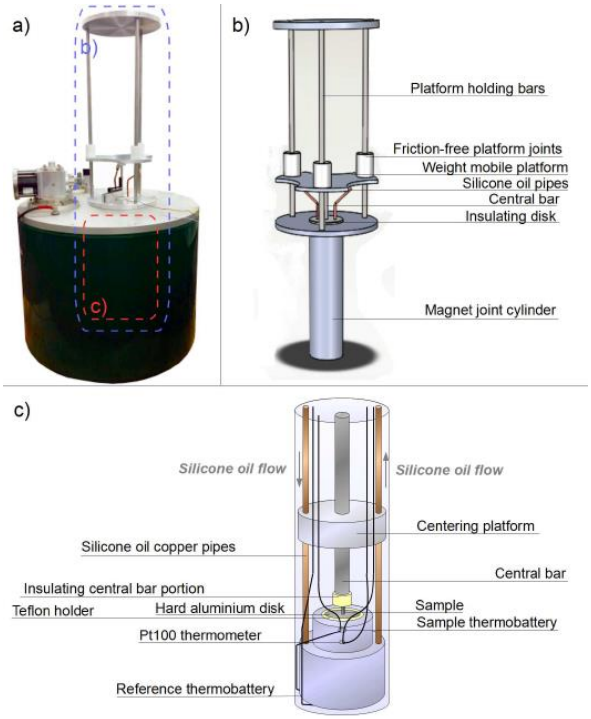

Fig. 3 a) picture of the cryogenic-free magnetic. The experimental setup is coupled to the bore of the magnet. b) and c) show different sections of the experimental setup. Extracted from [3]

A *Lauda Proline* thermal bath provides the thermal control of the calorimetric block by the silicone oil (*SIL 180*) which circulates through the copper pipes. The system has a mobile platform sustained by 3 bars, where in its surface, lead ingots are placed to apply uniaxial stress on the sample through the central bar connected to the mobile platform. A linear variable differential transformer (LVDT) in contact with the mobile platform measures the vertical linear displacement, X, of the dilation or contraction of the sample when the phase transition occurs. A 6T Cryogenic-Free Magnet controls the magnetic field applied and the calorimeter system is placed in the core of this magnet.

The sample is a Cu-Al-Zn shape memory alloy with a surface of 5,45 x 3,31 = 18,04mm², and a mass of 1,3847g. The Pt-100 of the calorimeter, the calorimetric signal and the LVDT are connected to their respective multimeters and computer controlled by *Labview* software.

A specific program within the *Lauda Proline* will run the bath temperature in a cooling-heating cycle from 60ºC to -15ºC with a ratio of 0,6 K/min while the electric signals of the sensors are recorded in the *Labview*. Each measurement is taken at a constant stress for a 5kg, 20kg, 40kg, 60kg, 80kg and 100kg weight. One last measurement with a 5T magnetic field and 5kg of weight is taken.

III. RESULTS & DISCUSSION

A. Calibration

We have taken 16 measurements in a range of the bath temperature from -40ºC to 110ºC. It is worth mention that, despite the fact of waiting long time for the system to reach a stable temperature, the bath temperature doesn't correspond to the temperature read by the Pt-100. A typical curve obtained in the calibration process is shown in Fig.4 at a 15ºC bath temperature.

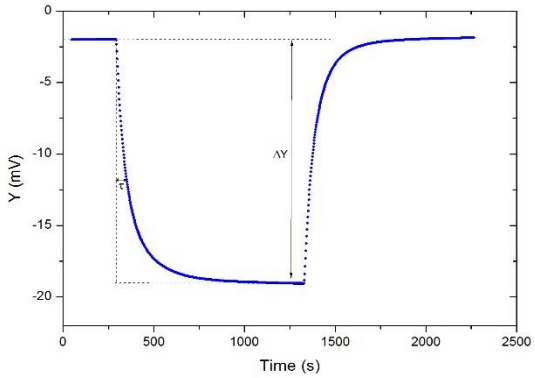

Fig. 4 Calibration thermogram showing the calorimetric output Y as a function of time where τ represents the response time parameter of the calorimeter. Bath temperature is 288K while the temperature of the Pt-100 is 291K.

The response time of the calorimeter is defined as the delay between the time a thermal event occurs and the corresponding stabilization of Y. In our case, this stabilization takes place exponentially $Y = SP(1 - e^{-\frac{t}{\tau}})$ and can be parametrized by the time constant τ. Fitting an exponential function to the corresponding region of the thermograms give us a value of $\boldsymbol{\tau \sim 71s}$ for our calorimeter.

The values obtained for the sensitivity at different temperatures are plotted in Fig. 5 Data can be fitted by the following third order polynomial:

$$S = -1{,}41 \cdot 10^{-5}T^3 + 0{,}01T^2 - 3{,}31T + 384{,}7$$

with a correlation of R^2=0,703

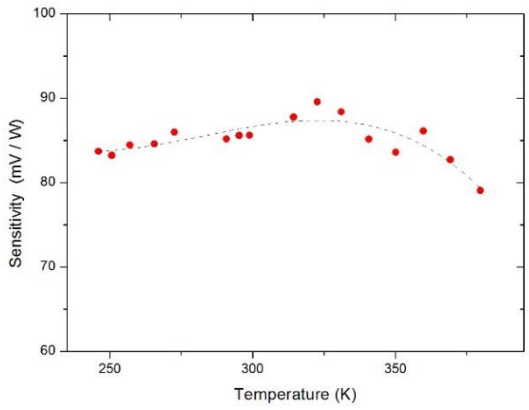

Fig. 5 Sensitivity as a function of temperature. The dash line is a third order polynomial fit to the data.

B. Differential Scanning calorimetry

The DSC measurements obtained for cooling and heating runs in a Cu-Zn-Al alloy are plotted in Fig. 6.

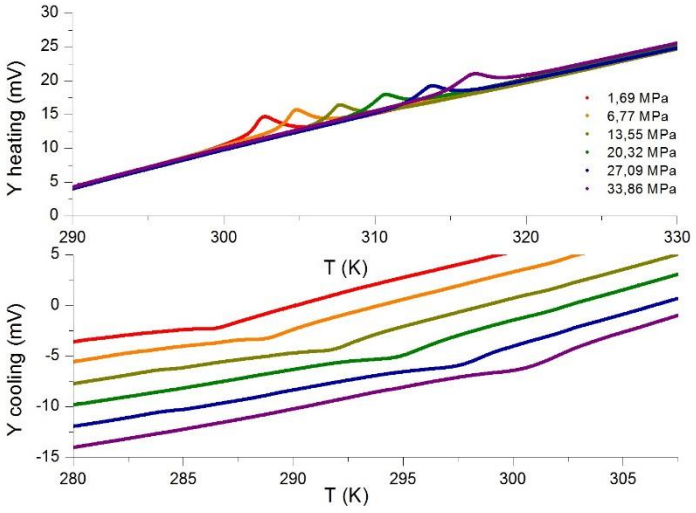

Fig. 6 Differential scanning calorimetry curves obtained for the Cu-Zn-Al sample in the heating and cooling runs for the different weigh applied: 5 kg, 20 kg, 40 kg, 60 kg, 80 kg and 100 kg. The cooling run curves have been arbitrarily vertically shifted to facilitate the visibility of the peaks in the graph. The stress corresponding to the weigh applied considering the surface of the sample is shown in the legend of the graph.

The peaks of the thermograms are associated with the large exothermal (upon cooling) and endothermal (upon heating) reactions of the martensitic transition.

It is observed in the graphics that the phase transition shifts to higher temperatures when increasing stress. This is due the application of uniaxial stress tends to drive the material to the monoclinic phase.

Fig. 7 shows the strain (cooling and heating runs) as a function of temperature for the different uniaxial stresses. It is noticed that, apart from the shift to higher temperatures, the transformation strain, ΔX, decreases with stress. Due the temperature range of the thermal bath, dilation of the central bar or the metal structure in general reduce the precision of the strain measurements.

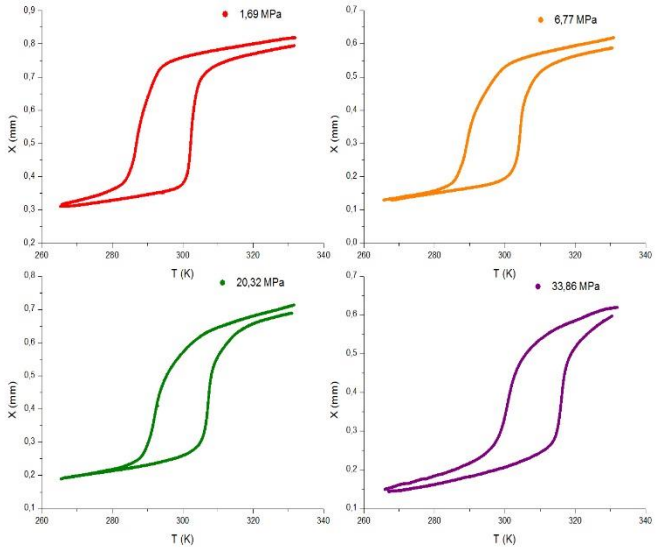

Fig. 7 Strain as a function of temperature in the heating and cooling runs for different stresses applied where X represents the displacement in millimetres.

A *Quick Basic* program has been used for the computation of the enthalpy and entropy changes from the data obtained by DSC. The program sets a proper baseline correction to correct from any asymmetric contribution of the calorimeter which is not related to the first-order transition and integrates numerically the thermogram peak for each stress. The computation has been done only for the heating run to minimize the error because the peaks appear considerably cleaner. The results obtained from the program are shown in Table 1 and plotted in Fig. 8.

σ (MPa)	T_p (K)	ΔS (J/kg·K^{-1})	ΔH (J/Kg·K^{-1})
1,69	303	22,35	6,63
6,77	305	17,49	5,49
20,32	308	16,71	5,72
13,55	311	18,42	6,88
27,09	314	11,35	4,36
33,66	317	13,52	5,79

Table 1. Results obtained from the *Quick Basic* program where T_p is the temperature of the peak, ΔS is the entropy change and ΔH is the enthalpy change.

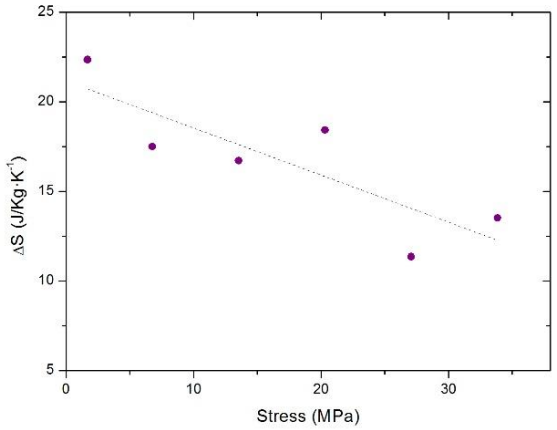

Fig. 8 Entropy change as a function of stress. The dashed line is a lineal fit to the data.

The plot shows how the entropy change decreases with stress. For this alloy, the entropy change is not expected to depend on the applied stress and the observed decrease is a consequence of a stress dependence of the sensitivity of the device.

C. Elastocaloric

Using the linear fit of the entropy vs. stress, we have implemented a correction of the entropy values obtained to compute the elastocaloric curves shown in Fig. 9.

The stress-induced entropy change vs temperature curves exhibit a plateau over a temperature interval. The value of this plateau is compatible with the transition entropy change, confirming that the giant elastocaloric effect is due to the martensitic transformation. The pronounced slope of the curves indicates that the phase transition takes place throughout the body of the material over a narrow temperature interval.

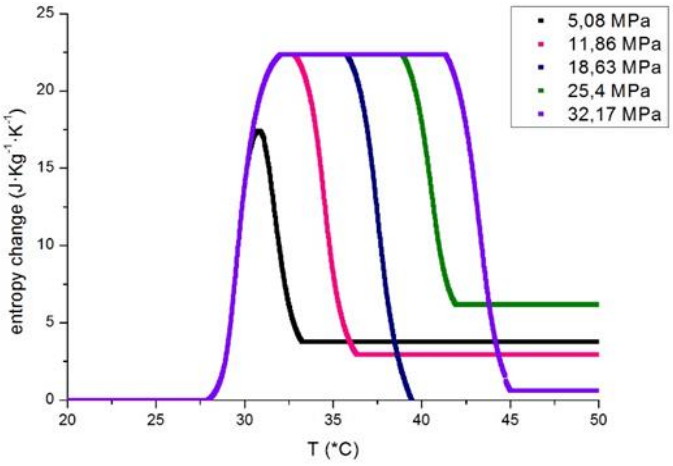

Fig 9 Entropy changes as a function of temperature for elastocaloric effect in Cu-Zn-Al at different values of the applied stress, $\Delta\sigma$. Where $\Delta\sigma = \sigma_i - \sigma_{5Kg}$

We obtain a maximum value for the stress-induced entropy change of 22,35 J/kg·K^{-1} within the temperature range between 32ºC and 41ºC and an applied stress of 32,17 MPa.

IV. CONCLUSIONS

- We have studied the elastocaloric properties of a Cu-Zn-Al sample. To do so, a calorimeter capable to work under uniaxial stress and magnetic field has been calibrated and differential scanning calorimetry technique has been implemented to measure the entropy change of the first-order phase transition.
- One measurement with a 5T magnetic field has been taken to verify that the sample and our experimental setup are not affected by magnetic fields.
- Results for the elastoccaloric effect obtained here from quasi-direct methods using calorimetry under stress are consistent with indirect results reported in the literature. [5].
- Elastocaloric effect is potentially useful for environmentally friendly refrigeration. Indeed, the elastocaloric effect has recently been identified as the most promising candidate to substitute the actual vapor-compression technologies, which require green-house gases that are harmful to the environment. The cooling capacity and the fact that his transition temperature is close to the room temperature make Cu-Zn-Al a promising material to be used in solid-state refrigeration devices.

Acknowledgments

The author gratefully acknowledges the support of the tutor and advisor Prof. Lluís Mañosa, without which the present study could not have been completed. The author would like to convey thanks to Adrià Gràcia for the help, support and patience he has placed in all this time. Last but not least, I also thank all friends and family who have helped and supported me, life and cosmos.

[1] Lluís Mañosa, Sergio Jarque-Farnos, Eduard Vives, and Antoni Planes, «Large temperature span and giant refrigerant capacity in elastocaloric Cu-Zn-Al shape memory alloys», *Applied Physics Letters 103, 211904* ,2013,Barcelona.

[2] Lluís Mañosa, Antoni Planes and Mehmet Acet, «Advanced materials for solid-state refrigeration», *J. Mater. Chem. A, 2013, 1,4925*, 2013

[3] Enric Stern i Taulats, «Giant caloric effects in the vicinity of first-order phase transitions», *PhD Thesis Universitat de Barcelona,* 2017

[4] Lluís Mañosa, Marc Bou, Carme Calles and Albert Cirera, «Low-cost differential scanning calorimeter», *American Journal of Physics vol. 64, No. 3,* 1996

[5] Jaka Tusek, Kurt Engelbrecht, Rubén Millán-Solsona, Lluís Mañosa, Eduard Vives, Lars P. Mikkelsen and Nini Pryds, «The Elastocaloric Effect: A Way to Cool Efficiently», *Advanced Energy Materials 1500361* DOI: 10.1002/aenm.201500361, 2015